Disorder-induced coherent pulses in direct-current driven external-cavity laser arrays

Greggory Scranton[1], Kendall Golden[2], Olivier Spitz[1], Arindam Mishra[1], Igor Belykh[2], and Yehuda Braiman[1]
[1] *The College of Optics and Photonics (CREOL), University of Central Florida, Orlando, FL 32816, USA*
[2] *Department of Mathematics and Statistics and Neuroscience Institute, Georgia State University, P.O. Box 4110, Atlanta, Georgia, 30302-410, USA*
(Dated: October 3, 2024)

The generation of high-power controlled pulses in semiconductor lasers and laser arrays is of significant theoretical and practical importance, with broad applications across various fields. The widespread view suggests that external factors, such as strong modulation, unilateral injection, or saturable absorbers, are necessary for pulse generation. In contrast, we demonstrate that direct-current-driven external-cavity laser arrays, subject only to optical feedback and non-local time-delayed coupling, can generate frequency disorder-induced pulsing without any external means. We establish how designed frequency disorder promotes coherent pulsing across the laser array at a high-bias current. This pulsing is characterized by highly desired features such as multi-GHz frequency operation, high peak power, and near-perfect phase synchronization. Through analysis and numerical simulations, we reveal the pulse generation mechanism that originates from a disorder-induced saddle-node bifurcation, leading to energy accumulation preceding pulse emission. Our breakthrough results pave the way for a new paradigm in the understanding and systematic design of disorder-induced controllable pulses for large, scalable semiconductor laser arrays.

Introduction. Semiconductor lasers are renowned for excitability under various perturbations that disturb their steady operation, with pulsing being particularly important for applications including optical neurons [1, 2] and photonics processors [3]. Studies across diverse platforms, from single lasers to 2D arrays, have shown that external means, such as AC driving [4], strong modulation [5, 6], or unilateral injection [7–11], play a key role in the controllable pulsing dynamics. For example, large amplitude modulation can trigger gain-switched pulses down to tens of picoseconds [12–17], and further pulse narrowing is achievable through mode locking, especially with a saturable absorber [18–24]. These external methods aimed to achieve nearly perfectly controllable pulsing dynamics [25, 26], in contrast to what is obtained with external optical feedback alone [27–31]. Despite some progress in generating pulses in laser arrays, synchronization between pulsing emitters with external control remains elusive. Pulses often propagate spatially rather than occurring simultaneously across the array [32–34]. Configurations with two lasers subject to both transverse coupling and optical feedback showed limited success in achieving synchronous pulsing [35, 36], and scalability for large arrays is still a significant challenge [37, 38].

Synchronization in laser arrays has been extensively studied [39–50], with intrinsic disorder and noise often regarded as disruptive factors. However, since the discovery that disorder can tame spatiotemporal instabilities and induce synchronization in oscillator networks [51, 52], it has been shown, both theoretically and experimentally, that under certain conditions, disorder-induced synchronization and coherent dynamics can emerge across a wide range of physical and engineering systems [53–59]. Notably, it has been demonstrated that a time-delayed laser array with inherent disorder, composed of broad-area diodes in an external V-shaped cavity, under the right conditions can achieve perfect synchrony [60–62]. Specifically, while frequency disorder typically degrades phase synchrony, the introduction of misalignment (disorder in time delays) can completely reverse this effect, leading to nearly perfect phase-synchronized behavior [62].

In this Letter, we demonstrate that contrary to the widespread assumption that external means are required for controllable pulsing, large arrays of semiconductor lasers subject to optical feedback and non-local delayed coupling can exhibit robust, high-power, coherent, and periodic pulsing dynamics at multi-GHz frequencies. Remarkably, this coherent pulsing is induced by an engineered frequency detuning disorder between emitters without the need for any external control mechanisms. This behavior sharply contrasts with the expected dynamics of single semiconductor lasers without external means. In our setting, the engineered pulsing features narrow time widths of tens of picoseconds, tunable intervals between well-separated single and multiple spike trains, and transition from anti-phase locking to phase locking, indicating the potential for coherent beam combining. By combining analytical techniques and numerical simulations, we uncover the underlying mechanism responsible for disorder-induced pulse generation in arrays of Lang-Kobayashi laser models. Our findings highlight the promise of engineered, all-optical pulsing in large semiconductor laser arrays, offering a clear path toward phase-locked beam combining for high-power optical pulse generation.

The laser array model. We consider a large array of Q delay-coupled semiconductor lasers with decayed non-

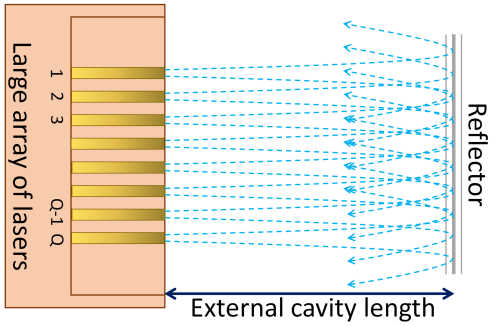

FIG. 1. Array of semiconductor lasers subject to decayed non-local coupling and optical feedback. The feedback and decayed coupling provided by the external reflector. The reflected beam from each emitter couples to the other lasers in the array after a time delay τ.

local coupling described by a version [62] of the Lang-Kobayashi equations [63]:

$$\begin{aligned}\dot{E}_q(t) &= \tfrac{1+i\alpha}{2}\left(g\tfrac{N_q(t)-N_0}{1+s|E_q(t)|^2}-\gamma\right)E_q(t)+\\ &\quad i\sigma\omega_q E_q(t)+\tfrac{\kappa^f}{Q}\sum_{j=1}^{Q}A_{qj}(E_j(t-\tau))\\ \dot{N}_q(t) &= \beta J_{th}-\gamma_n N_q(t)-g\tfrac{N_q(t)-N_0}{1+s|E_q(t)|^2}|E_q(t)|^2,\end{aligned} \tag{1}$$

with the qth laser complex field $E_q(t) = r_q(t)\exp i\phi_q(t)$ and carrier number $N_q(t)$. The parameters are customary for Lang-Kobayashi-type models: g and N_0 are the differential gain coefficient and number of carriers at transparency, respectively, γ is the cavity loss rate, $J_{th} = \gamma_n\left[N_0 + (\gamma/g)\right]$ is the pump current threshold, the pump factor $\beta > 1$ means that the lasers are biased above threshold, γ_n is the carrier loss rate, κ^f is the feedback strength. The frequency detuning of the qth laser is ω_q. The time delay τ is the external cavity round trip time which is identical for all lasers. $A_{qj} = d^{|q-j|} \in (0,1)$ is the entry of the decay non-local coupling matrix connecting the qth laser to the jth laser. Although we have computationally verified the emergence of pulses even in the presence of noise and/or non-identical time delays, we have not considered noise and misalignment disorder effects here to explain the pulsing mechanism better and facilitate comparison with the reduced model. Supplementary Table 1 contains the full set of the parameter values and their meaning. Figure 1 schematically illustrates the laser array (1) with $Q = 8$ emitters.

Previous studies within the Lang-Kobayashi framework for a single laser have extensively reported on the dynamical routes to chaos, including stable locking, switching dynamics (particularly in short-cavity regimes [64, 65]) and periodic oscillations [66, 67]. However, these studies have only documented switching dynamics rather than the distinct single-pulse or multi-pulse operation reported in this Letter (see the Supplementary Material for possible single-laser non-pulsing dynamics). We will also emphasize that pulsing conditions are encountered for moderate-to-strong feedback strengths and bias currents high above thresholds. The latter differs from most of the pulsing schemes with external means mentioned above, which require the laser to be biased close to the threshold to optimize the pulse characteristics.

Numerical simulations. For a large array of 30 semiconductor lasers, intensity time traces of pulsing are shown in Fig. 2. Several conditions of operation are highlighted to prove the tunability of the pulsing pattern, with a single pulse per period Fig. 2 (a), three pulses per period in Fig. 2 (b), and four pulses per period in Fig. 2 (c), with the peculiarity, in the latter, that the time interval between each pulse differs inside a train of pulse. The periodicity of pulses and pulse trains is very close to the external cavity time delay τ. There can be up to three characteristic time scales (one for cavity roundtrip time, one for intervals between pulse trains, and one for intervals between the pulses within a single pulse train) at stake in this nonlinear phenomenon. Figure 2 shows two distinct pulsing dynamics within the array, with even-numbered lasers exhibiting one pattern and odd-numbered lasers displaying another pattern. This stems from the choice of frequency detuning presented in this study (2 GHz for even lasers and -2 GHz for odd lasers). This choice of detuning helps illustrate the pulsing mechanism, but does not contrast strongly with other pulsing configurations detailed in the Supplementary Material. This detuning configuration was engineered to better enable pulsing, although other non-alternating detuning configurations can also induce pulsing.

Figure 3 provides a more detailed view of the overall behavior of the 30-laser array. In the single-pulse case, as shown in Fig. 3(a), the lasers exhibit alternating dynamics: even-numbered lasers follow a similar pulsing pattern, while odd-numbered lasers share a distinct, yet comparable behavior. The only notable deviation occurs at the edges of the array, where the network interactions are slightly different, resulting in less pronounced pulsing. Figure 3(b) details the evolution of coherence over time, displaying the combined field intensity (black curve) and the Kuramoto order parameter in the inset (blue curve). The combined field intensity is given by: $\mathcal{C}(t) = |\sum_{q=1}^{Q} E_q(t)|^2$. This metric complements the complex Kuramoto order parameter [68, 69], which is defined as $R(t)e^{i\Phi(t)} = \frac{1}{Q}\sum_{q=1}^{Q}\exp\left(i\phi_q(t)\right)$ and reaches 1 when all lasers are in-phase synchronized and 0 when they are anti-phase synchronized. For comparison, the green curve represents the intensity of one of the even lasers, scaled by 30^2, while the orange curve shows the intensity of one of the odd lasers, similarly scaled. A notable feature is the pronounced dip in the combined field intensity, which occurs when the even-numbered lasers pulse. At the dip's lowest point, the lasers are anti-phase synchronized. A few tens of picoseconds later, the odd-

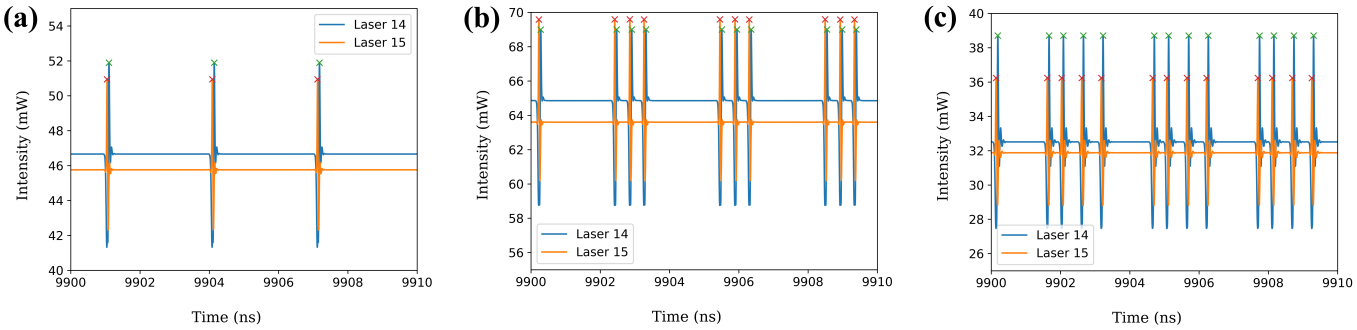

FIG. 2. Periodic pulsing dynamics in a 30-laser array under various operating conditions after discarding transients. (a) Single pulse behavior, parameters $\beta = 6.75$, $\kappa^f = 45ns^{-1}$. (b) Triple pulse behavior, parameters $\beta = 9.0$, $\kappa^f = 44.8ns^{-1}$. (c) Quadruple pulse behavior with varying time intervals between pulses, parameters $\beta = 5.0$, $\kappa^f = 43.2ns^{-1}$. In each panel, the blue trace represents laser #14, exhibiting the typical behavior of even-numbered lasers, while the orange trace shows laser #15, reflecting the behavior of odd-numbered lasers. Crosses indicate the detected peaks in the time traces.

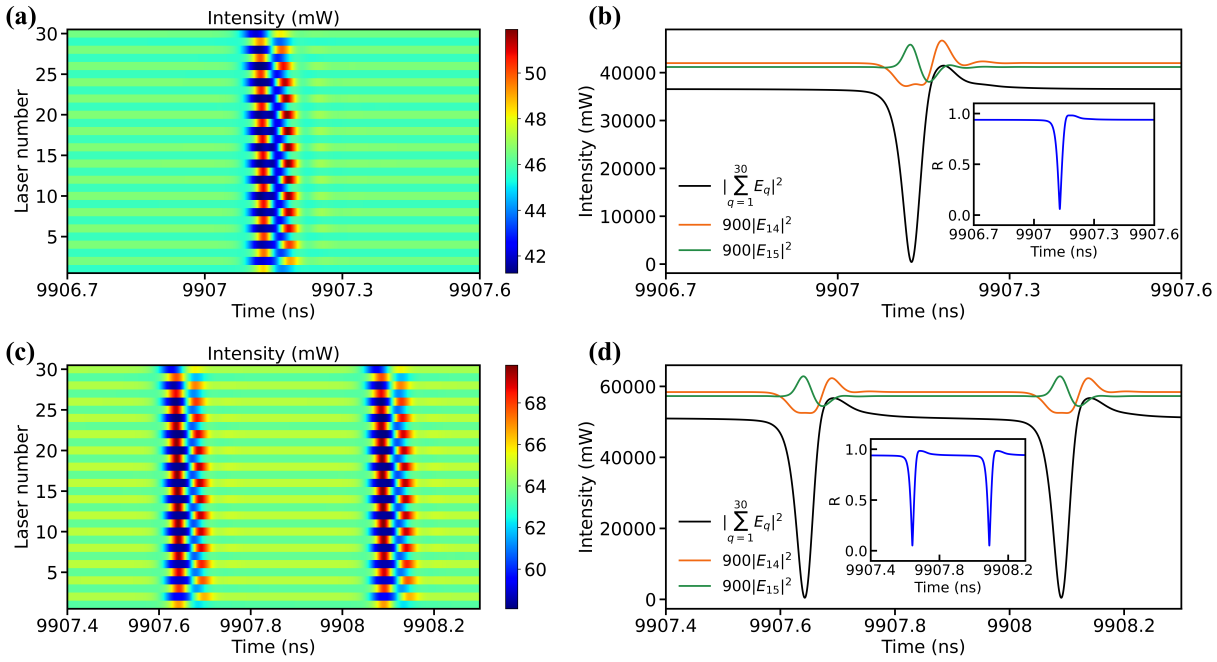

FIG. 3. (a) Heatmap of single-pulse dynamics in a 30-laser array with distinct behaviors between odd and even lasers. (b) Combined field intensity (black curve) of the 30 lasers, highlighting anti-phase and in-phase synchronization periods. The panel also shows the magnified intensity of an odd laser (green curve) and an even laser (orange curve). The inset demonstrates the Kuramoto order parameter $R(t)$, confirming transitions between anti-phase and in-phase synchrony. The parameters for this case are $\beta = 6.75$, $\kappa^f = 45ns^{-1}$. (c-d) Same as (a)-(b) but for a pattern with two pulses per period, parameters $\beta = 9.0$, $\kappa^f = 45ns^{-1}$.

numbered lasers pulse in phase with the Kuramoto order parameter approaching 1. This alternating pattern between even and odd-numbered lasers persists when the system is configured for two pulses per period, as seen in Fig. 3(c)-(d), with a strong dip triggered when the even lasers are pulsing. In all other multi-pulsing cases, including those shown in Fig. 2, the pattern remains consistent (not shown). The number of dips in the combined field intensity matches the number of pulses per period, and the Kuramoto order parameter remains high (above 96 %) when the odd-numbered lasers are pulsing. Notably, very similar pulsing dynamics are persistent when random perturbations are added to the frequency-detuning values. Supplementary Table 2 gives an example of perturbed detunings that preserve pulsing similar to what is shown in Fig. 3. Unlike other laser networks, particularly those using saturable absorbers, pulsing in our array occurs simultaneously across all lasers without spatial propagation over time. This results in high phase synchrony during the pulsing state, which is advantageous

for beam combining. Achieving nearly perfect coherence is particularly relevant in large laser arrays, as optical power scales with the square of the number of emitters along the propagation axis.

Disorder-induced mechanism for pulse generation. To understand the underpinnings of the disorder-induced pulsing without confounding factors, we consider the minimal laser array (1) with $Q = 2$ and $d = 1$, which can be cast into the polar coordinate form for laser field $E_q(t)$:

$$\begin{aligned}
\dot{r}_q &= Gr_q(t) + \tfrac{\kappa^f}{2} \sum_{j=1}^{2} r_j(t-\tau)\cos\left(\phi_j(t-\tau) - \phi_q(t)\right), \\
\dot{\phi}_q &= \alpha G + \omega_q + \tfrac{\kappa^f}{2} \sum_{j=1}^{2} \tfrac{r_j(t-\tau)}{r_q(t)} \sin\left(\phi_j(t-\tau) - \phi_q(t)\right), \\
\dot{N}_q &= J_0 - \gamma_n N_q - 2gG(r_q, N_q) r_q^2, \; q = 1, 2,
\end{aligned} \tag{2}$$

where function $G = \frac{1}{2}\left(g\frac{N_q(t)-N_0}{1+sr_q^2(t)} - \gamma\right)$, $r_q(t)$, and $\phi_q(t)$ are the complex field magnitude and phase, respectively. We aim to derive an analytically tractable model that explicitly demonstrates how rapid periodic phase destabilization originating from the frequency detuning can induce pulsing. Our simulations of the array (2) detailed in Supplementary Fig. 5 indicate that (i) the period of coherent pulsing is nearly constant and close to the time-delay τ and (ii) $r_1(t)$ and $N_1(t)$ are close to $r_2(t)$ and $N_2(t)$ at the nearly coherent state. Therefore, we approximate $r_1(t-\tau) \approx r_1(t) \approx r_2(t-\tau) \approx r_2(t) \equiv r(t)$, $\phi_1(t-\tau) \approx \phi_1(t)$, $\phi_1(t-\tau) \approx \phi_1(t)$, and $N_1(t-\tau) \approx N_1(t) \approx N_2(t-\tau) \approx N_2(t) \equiv N(t)$, where $r(t)$ and $N(t)$ correspond to a nearly coherent state. We then introduce the phase difference $\theta = \phi_1 - \phi_2$ whose evolution is governed by $\dot{\theta} = \Delta\omega + \frac{\kappa^f}{2}(\sin\left(\phi_2(t-\tau) - \phi_1(t)\right) - \sin\left(\phi_1(t-\tau) - \phi_2(t)\right)$, where $\Delta\omega = \omega_1 - \omega_2$ is a frequency detunning. Applying the trigonometric identity for the difference of sines, we simplify the θ equation and obtain the reduced system that approximately describes the collective dynamics close to the coherent state:

$$\begin{aligned}
&\dot{r} = Gr + \frac{\kappa^f}{2}(1+\cos\theta)r(t), \quad \dot{\theta} = \Delta\omega - \kappa^f \sin\theta, \\
&\dot{N} = J_0 - \gamma N(t) - 2gGr^2.
\end{aligned} \tag{3}$$

Note that the phase difference equation does not contain r and N and represents a nonuniform phase oscillator [70]. This equation has two fixed points that disappear when $\Delta\omega$ exceeds κ^f. Under the condition that $\Delta\omega$ is slightly greater than κ^f, θ slowly drifts near a ghost state, emerging from a saddle-node bifurcation at $\Delta\omega = k^f$, before rapidly completing the cycle. This rapid increase in the phase difference with θ reaching π destabilizes the r equation via the increased positive term $(1+\cos\theta)$ and induces a pulse in r. The time between the pulses is determined by the nonuniform oscillator's period $T_{period} = 2\pi/\sqrt{\Delta\omega^2 - (k^f)^2}$ [70], where the denominator is small. Figure 4 shows that the reduced model (3) predicts the onset of coherent single-pulse dynamics in the full model (2) via the disorder-induced saddle-node bifurcation remarkably well. Note that the reduced system (3) was derived under the close zero-order approximation that the pulsing periodicity is precisely equal to the external cavity time delay. Therefore, it can only capture single-pulse dynamics, not multi-pulse trains whose characterization requires higher-order perturbation analysis.

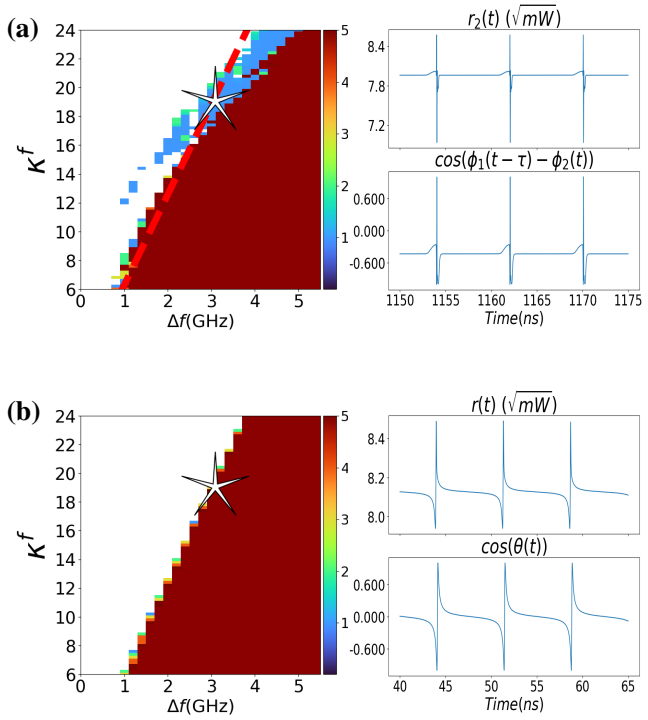

FIG. 4. Pulse generation in the two-laser array (2) (a) and its reduced model (3) (b) as a function of the frequency detuning, $\Delta f = \Delta\omega/2\pi$, and feedback coupling strength, κ^f (in ns^{-1}). The color in the heatmaps (left panels) indicates the number of peaks per time period $T = \tau = 8$ ns. The blue region shows one-pulse dynamics, calculated over 100 trials in (a) to account for multistability and one trial in (b), all from random initial conditions. The white and dark red regions correspond to the lasers' steady operation and fast oscillatory behavior, respectively. The red dashed curve in (a) represents the reduced model's saddle-node bifurcation curve $\kappa^f = \Delta\omega$ that adequately predicts the pulse generation boundary in (2). Note the gap on the x-axis highlighting the non-zero minimal frequency detuning required to induce pulsing at $\Delta f^* \approx 0.9$ GHz. The white star (left panels) and accompanying time traces (right panels) correspond to $\Delta f = 3.027$ GHz and $\kappa^f = 19$ ns^{-1}. Only the r_2 time series is plotted in (a), with nearly coherent $r_1(t)$ similar to Fig. 2(a) [not shown]. Parameters for these runs are shown in Supplementary Table 3.

Conclusions. We demonstrated that direct-current-driven external-cavity laser arrays, relying solely on optical feedback and non-local time-delayed coupling, can generate periodic, coherent, high-power and high-

frequency pulses and pulse trains. We have uncovered the pulse generation mechanism originating from a disorder-induced saddle-node bifurcation, facilitating energy accumulation for subsequently triggering the emission of pulses. Pulse characteristics depend on diode array detuning patterns so that pulses could be experimentally realized and controlled by engineering frequency detunings via, e.g., individual control of bias currents or other means. Our approach opens new avenues for practical applications, including high-power pulse beam combining and neuromorphic optical computing. Furthermore, the disorder-induced mechanism of coherent pulse generation promises to have substantial implications beyond laser arrays, extending to other excitable physical and biological systems.

Acknowledgements. This work is supported by the Office of Naval Research. The authors thank Mark A. Berrill for his help in developing optimized numerical tools for the time-delayed system simulations and Matthew Crespo for his initial work on the topic of pulsing laser arrays.

[1] P. R. Prucnal, B. J. Shastri, T. Ferreira de Lima, M. A. Nahmias, and A. N. Tait, Advances in Optics and Photonics **8**, 228 (2016).
[2] J. Robertson, E. Wade, Y. Kopp, J. Bueno, and A. Hurtado, IEEE Journal of Selected Topics in Quantum Electronics **26**, 1 (2019).
[3] M. Nakajima, K. Tanaka, and T. Hashimoto, Communications Physics **4**, 20 (2021).
[4] M. Zbik, in *CLEO: Applications and Technology* (Optica Publishing Group, 2019) pp. AF3K–7.
[5] B. Liu, Y. Braiman, N. Nair, Y. Lu, Y. Guo, P. Colet, and M. Wardlaw, Optics Communications **324**, 301 (2014).
[6] O. Spitz, S. Koyu, M. Berrill, and Y. Braiman, in *2023 IEEE Photonics Conference (IPC)* (IEEE, 2023) pp. 1–2.
[7] J. R. Tredicce, F. T. Arecchi, G. L. Lippi, and G. P. Puccioni, JOSA B **2**, 173 (1985).
[8] S. Wieczorek, B. Krauskopf, and D. Lenstra, Physical Review Letters **88**, 063901 (2002).
[9] S. Wieczorek, B. Krauskopf, T. B. Simpson, and D. Lenstra, Physics Reports **416**, 1 (2005).
[10] D. Goulding, S. P. Hegarty, O. Rasskazov, S. Melnik, M. Hartnett, G. Greene, J. G. McInerney, D. Rachinskii, and G. Huyet, Physical Review Letters **98**, 153903 (2007).
[11] B. Kelleher, C. Bonatto, G. Huyet, and S. P. Hegarty, Physical Review E **83**, 026207 (2011).
[12] P. Downey, J. Bowers, R. Tucker, and E. Agyekum, IEEE Journal of Quantum Electronics **23**, 1039 (1987).
[13] P. Paulus, R. Langenhorst, and D. Jager, IEEE journal of quantum electronics **24**, 1519 (1988).
[14] H.-F. Liu, M. Fukazawa, Y. Kawai, and T. Kamiya, IEEE Journal of Quantum Electronics **25**, 1417 (1989).
[15] J. Karin, L. Melcer, R. Nagarajan, J. Bowers, S. Corzine, P. Morton, R. Geels, and L. Coldren, Applied Physics Letters **57**, 963 (1990).
[16] T. Wicht, S. Schuster, H. Haug, J. Sacher, M. Hofmann, W. Elsasser, and E. O. Gobel, IEEE journal of quantum electronics **27**, 1682 (1991).
[17] P. Täschler, L. Miller, F. Kapsalidis, M. Beck, and J. Faist, Optica **10**, 507 (2023).
[18] H. Haus, IEEE Journal of Quantum Electronics **11**, 323 (1975).
[19] H. A. Haus, Journal of Applied Physics **46**, 3049 (1975).
[20] H. Wünsche, O. Brox, M. Radziunas, and F. Henneberger, Physical review letters **88**, 023901 (2001).
[21] S. Barbay, R. Kuszelewicz, and A. M. Yacomotti, Optics Letters **36**, 4476 (2011).
[22] D. Revin, M. Hemingway, Y. Wang, J. Cockburn, and A. Belyanin, Nature Communications **7**, 11440 (2016).
[23] X. Liu and Y. Cui, Advanced Photonics **1**, 016003 (2019).
[24] M. Roy, Z. Xiao, C. Dong, S. Addamane, and D. Burghoff, Optica **11**, 1094 (2024).
[25] M. Turconi, B. Garbin, M. Feyereisen, M. Giudici, and S. Barland, Physical Review E **88**, 022923 (2013).
[26] J. Tiana-Alsina, B. Garbin, S. Barland, and C. Masoller, Chaos: An Interdisciplinary Journal of Nonlinear Science **30**, 081101 (2020).
[27] D. W. Sukow, J. R. Gardner, and D. J. Gauthier, Physical Review A **56**, R3370 (1997).
[28] A. M. Yacomotti, M. C. Eguia, J. Aliaga, O. E. Martinez, G. B. Mindlin, and A. Lipsich, Physical Review Letters **83**, 292 (1999).
[29] J. A. Reinoso, J. Zamora-Munt, and C. Masoller, Physical Review E **87**, 062913 (2013).
[30] B. Garbin, J. Javaloyes, G. Tissoni, and S. Barland, Nature Communications **6**, 5915 (2015).
[31] O. Spitz, J. Wu, A. Herdt, G. Maisons, M. Carras, W. Elsäßer, C.-W. Wong, and F. Grillot, Advanced Photonics **2**, 066001 (2020).
[32] D. Puzyrev, A. Vladimirov, A. Pimenov, S. Gurevich, and S. Yanchuk, Physical Review Letters **119**, 163901 (2017).
[33] K. Alfaro-Bittner, S. Barbay, and M. Clerc, Chaos: An Interdisciplinary Journal of Nonlinear Science **30** (2020).
[34] I. Simos, C. Simos, and N. A. Stathopoulos, JOSA B **39**, 2457 (2022).
[35] M. Münkel, F. Kaiser, and O. Hess, International Journal of Bifurcation and Chaos **8**, 951 (1998).
[36] A. Scirè, C. J. Tessone, and P. Colet, IEEE Journal of Quantum Electronics **41**, 272 (2005).
[37] K. Otsuka and J.-L. Chern, Physical Review A **45**, 5052 (1992).
[38] M. Münkel, F. Kaiser, and O. Hess, Physical Review E **56**, 3868 (1997).
[39] H. G. Winful and L. Rahman, Physical Review Letters **65**, 1575 (1990).
[40] T. Sugawara, M. Tachikawa, T. Tsukamoto, and T. Shimizu, Physical Review Letters **72**, 3502 (1994).
[41] R. Roy and K. S. Thornburg Jr, Physical Review Letters **72**, 2009 (1994).
[42] G. Kozyreff, A. Vladimirov, and P. Mandel, Physical Review E **64**, 016613 (2001).
[43] C. Masoller, Physical Review Letters **86**, 2782 (2001).
[44] Y. C. Kouomou, P. Colet, N. Gastaud, and L. Larger, Physical Review E **69**, 056226 (2004).
[45] J. Zamora-Munt, C. Masoller, J. Garcia-Ojalvo, and R. Roy, Physical Review Letters **105**, 264101 (2010).
[46] M. Nixon, M. Fridman, E. Ronen, A. A. Friesem, N. Davidson, and I. Kanter, Physical Review Letters **108**,

214101 (2012).
[47] F. Grillot, A. Gavrielides, O. Spitz, T. C. Newell, and M. Carras, in *Quantum Sensing and Nano Electronics and Photonics XV*, Vol. 10540 (SPIE, 2018) pp. 224–231.
[48] J. Ding, I. Belykh, A. Marandi, and M.-A. Miri, Physical Review Applied **12**, 054039 (2019).
[49] J. Sheng, X. Wei, C. Yang, and H. Wu, Physical Review Letters **124**, 053604 (2020).
[50] J. Hillbrand, D. Auth, M. Piccardo, N. Opačak, E. Gornik, G. Strasser, F. Capasso, S. Breuer, and B. Schwarz, Physical Review Letters **124**, 023901 (2020).
[51] Y. Braiman, J. F. Lindner, and W. L. Ditto, Nature **378**, 465 (1995).
[52] Y. Braiman, W. Ditto, K. Wiesenfeld, and M. Spano, Physics Letters A **206**, 54 (1995).
[53] T. Nishikawa and A. E. Motter, Physical Review Letters **117**, 114101 (2016).
[54] J. D. Hart, Y. Zhang, R. Roy, and A. E. Motter, Physical Review Letters **122**, 058301 (2019).
[55] K. Daley, K. Zhao, and I. V. Belykh, Chaos: An Interdisciplinary Journal of Nonlinear Science **30** (2020).
[56] Y. Zhang, J. L. Ocampo-Espindola, I. Z. Kiss, and A. E. Motter, Proceedings of the National Academy of Sciences **118**, e2024299118 (2021).
[57] F. Molnar, T. Nishikawa, and A. E. Motter, Nature Communications **12**, 1457 (2021).
[58] N. Punetha and L. Wetzel, Physical Review E **106**, L052201 (2022).
[59] Y. Eliezer, S. Mahler, A. A. Friesem, H. Cao, and N. Davidson, Physical Review Letters **128**, 143901 (2022).
[60] B. Liu and Y. Braiman, Optics Express **21**, 31218 (2013).
[61] B. Liu, Y. Liu, and Y. Braiman, Optics Express **16**, 20935 (2008).
[62] N. Nair, K. Hu, M. Berrill, K. Wiesenfeld, and Y. Braiman, Physical Review Letters **127**, 173901 (2021).
[63] R. Lang and K. Kobayashi, IEEE journal of Quantum Electronics **16**, 347 (1980).
[64] T. Heil, I. Fischer, W. Elsäßer, B. Krauskopf, K. Green, and A. Gavrielides, Physical Review E **67**, 066214 (2003).
[65] A. Tabaka, K. Panajotov, I. Veretennicoff, and M. Sciamanna, Physical Review E **70**, 036211 (2004).
[66] C. Masoller, Chaos: An Interdisciplinary Journal of Nonlinear Science **7**, 455 (1997).
[67] J.-X. Dong, J. Ruan, L. Zhang, J.-P. Zhuang, and S.-C. Chan, Physical Review A **103**, 053524 (2021).
[68] J. A. Acebrón, L. L. Bonilla, C. J. Pérez Vicente, F. Ritort, and R. Spigler, Reviews of Modern Physics **77**, 137 (2005).
[69] D. Kazakov, N. Opačak, F. Pilat, Y. Wang, A. Belyanin, B. Schwarz, and F. Capasso, APL Photonics **9** (2024).
[70] S. H. Strogatz, *Nonlinear dynamics and chaos: with applications to physics, biology, chemistry, and engineering* (CRC press, 2018).